

Ubiquitous increases in flood magnitude in the Columbia River Basin under climate change

Laura E. Queen¹, Philip W. Mote¹, David E. Rupp¹, Oriana Chegwiddden², and Bart Nijssen²

¹Oregon Climate Change Research Institute, Oregon State University, Corvallis OR 97331 USA

²Department of Civil and Environmental Engineering, University of Washington Seattle WA 98105 USA

Correspondence to: Laura Queen (lqueen@uoregon.edu)

Abstract. The US and Canada have entered negotiations to modernize the Columbia River Treaty, signed in 1961. Key priorities are balancing flood risk, hydropower production, and improving aquatic ecosystem function while incorporating projected effects of climate change. In support of the US effort, Chegwiddden et al. (2017) developed a large-ensemble dataset of past and future daily flows at 396 sites throughout the Columbia River Basin (CRB) and select other watersheds in western Washington and Oregon, using state-of-the art climate and hydrologic models. In this study, we use that dataset - the largest now available - to present new analyses of the effects of future climate change on flooding using water year maximum daily flows. For each simulation, flood statistics are estimated from Generalized Extreme Value distributions fit to simulated water year maximum daily flows for 50-year windows of the past (1950-1999) and future (2050-2099) periods. Our results contrast with previous findings: we find that the vast majority of locations in the CRB are estimated to experience an increase in future discharge magnitudes. We show that on the Columbia and Willamette rivers, increases in discharge magnitudes are smallest downstream and grow larger moving upstream. For the Snake River, however, the pattern is reversed, with increases in discharge magnitudes growing larger moving downstream to the confluence with the Salmon River tributary, and then abruptly dropping. We decompose the variation in results attributable to variability in climate and hydrologic factors across the ensemble, finding that climate contributes more variation in larger basins while hydrology contributes more in smaller basins. Equally important for practical applications like flood control rule curves, the seasonal timing of flooding shifts dramatically on some rivers (e.g., on the Snake, 20th century floods occur exclusively in late spring, but by the end of the 21st century some floods occur as early as December) and not at all on others (e.g. the Willamette).

29 **1 Introduction**

30 Among natural disasters in the Northwest, flooding ranks second behind fire in federal disaster declarations¹ since
31 1953 despite extensive flood prevention infrastructure. The largest flood in modern times on the Columbia oc-
32 curred in late spring (May-June) 1948, and obliterated the town of Vanport which lay on an island between Port-
33 land, OR and Vancouver, WA, permanently displacing its 18,500 residents². Other disruptive floods in the region
34 include the Heppner flood in 1903, one of the deadliest flash floods in US history (Byrd, 2014); floods on the
35 Chehalis River in both December 2007³ and January 2009⁴ that closed Interstate 5, the main north-south trans-
36 portation corridor through the Northwest, for several days each time at a cost of several \$m per day to freight
37 movement alone; and floods on the Willamette River in February 1996 and April 2019. The timing of typical
38 floods varies widely across the region: low-elevation basins in western Washington and Oregon typically flood
39 in November through February, whereas the snow-dominant basins east of the Cascades more typically flood in
40 spring, even as late as June (Berghuis et al. 2016).

41

42 The Columbia River drains much of the Northwest, with the fourth largest annual flow volume in the US and a
43 drainage that includes portions of seven states plus the Canadian province of British Columbia (BC), an area of
44 668,000 km² (Fig. 1). Its numerous federal and nonfederal dams provide flood protection, hydropower production,
45 navigation, irrigation, and recreation services. A treaty between the US and Canada, signed in 1961, codified joint
46 management of the river's reservoirs (and funded construction of new reservoirs in BC) primarily to provide flood
47 protection and hydropower production⁵. The US and Canada have entered negotiations to update the treaty; the
48 USA's "key objectives include continued, careful management of flood risk; ensuring a reliable and economical

¹ <https://www.fema.gov/data-visualization-summary-disaster-declarations-and-grants> accessed 8/6/2019

² https://www.oregonlive.com/portland/2017/05/vanport_flood_may_30_1948_chan.html accessed 8/6/2019

³ <https://www.seattletimes.com/seattle-news/extensive-flooding-3-confirmed-deaths-hundreds-of-rescues/> ac-
cessed 8/6/2019

⁴ [https://www.seattletimes.com/seattle-news/despite-drying-cooling-trend-flooding-and-road-closures-con-
tinue/](https://www.seattletimes.com/seattle-news/despite-drying-cooling-trend-flooding-and-road-closures-con-
tinue/) accessed 8/6/2019

⁵ <https://www.state.gov/columbia-river-treaty/> accessed 8/6/2019

49 power supply; and improving the ecosystem in a modernized Treaty regime.” (*ibid.*) Both countries have ex-
50 pressed an intention to include the effects of climate change on flows, and clearly a key aspect of hydrologic
51 change is to inform the treaty negotiations of the influence of climate change on the magnitude of flooding.

52

53

54 While rising temperatures potentially affect all parts of the hydrologic cycle, in a snowmelt-dominated hydrologic
55 system such as many of the Northwest’s river basins, warming directly affects snow accumulation and melt (e.g.,
56 Hamlet et al. 2005). Observational studies have shown consistent changes toward lower spring snowpack (Mote
57 et al. 2018), earlier spring flow (Stewart et al. 2005), and lower summer flow (Fritze et al. 2011) since the mid-
58 20th century. Observations of trends in flooding in the US have generally failed to find any consistent trends (Lins
59 and Slack 1999; Douglass et al. 2000; Sharma et al. 2018). Sharma et al. (2018) offer several possible explan-
60 ations, chiefly “decreases in antecedent soil moisture, decreasing storm extent, and decreases in snowmelt”. The
61 detection of trends in floods is complicated by the interaction of extreme events and nonstationarity (Serinaldi
62 and Kilsby, 2015). Moreover, as a result of the substantial alteration of rivers to prevent flooding (e.g., by the
63 construction of dams and levees) during the observational period, the best long-term records - i.e., on streams with
64 the least modifications - are on rivers that were not producing sufficiently disruptive floods to lead decision-
65 makers to construct flood protection structures. That is, as flooding of settlements, infrastructure, or other assets
66 led to the investments in flood protection structures on most rivers, thereby altering the flow regime and dividing
67 any gauged records into pre- and post- modification, the ones that were left unmodified tended to be small and/or
68 remote.

69

70 To interpret the ambiguous results from observed trends, Hamlet and Lettenmaier (2007) used the Variable Infil-
71 tration Capacity (VIC) hydrologic model forced twice with detrended observed daily weather for the period 1916-
72 2003, with about 1°C of temperature difference between the two. They then compared 20- and 100-year flood
73 quantiles for basins at varying sizes in the western US and found a wide range of changes in flood magnitude
74 ranging from large decreases to large increases (+/- 30%). Broadly, the responses depended somewhat on basin
75 winter temperature, with the coldest basins (<-6°C) showing reductions in flood magnitude owing to reduced
76 snowpack, basins with moderate temperatures exhibiting a wide range of changes, and rain-dominant (>5°C)
77 basins showing little change, though the warm basins in coastal areas of Washington, Oregon, and California
78 showed increased flood magnitude.

79

80 Modeling work using state-of-the-art hydrologic models has been applied to understand where and how flood
81 magnitudes may change in the future. Tohver et al (2014) found widespread increases in flood magnitudes, espe-
82 cially in temperature-sensitive basins (mainly on the west side of the Cascades), but their approach used monthly
83 GCM output so changes in daily precipitation would not be represented. Salathé et al. (2014) used a single global
84 climate model (GCM), the ECHAM5, linked to a regional climate model to obtain high-resolution (in space and
85 time) driving data for VIC over the period 1970-2069. As did Hamlet and Lettenmaier (2007), they compared the
86 ratio of flood change (2050s vs 1980s) against mean historical winter temperature and found a majority of loca-
87 tions with a higher 100-year flood, in some cases by a factor of 2 or more; while they projected increases in every
88 one of the warmer basins ($>0^{\circ}\text{C}$), a substantial fraction of colder locations had decreases in flood magnitude.

89

90 As noted above and detailed below, Chegwiddden et al. (2019) describe the process used to generate the streamflow
91 ensemble used here. In addition, they used analysis of variance (ANOVA) to analyze the different influences of
92 choices of emissions scenario (as a Representative Concentration Pathway - RCP), GCM, downscaling method,
93 and hydrologic model, and how those influences varied spatially across the domain and also seasonally and by
94 hydrologic variable. They found that the RCP and GCM had the largest influence on the range of annual stream-
95 flow volume and timing, and hydrologic model had the largest influence on low flows. The hydrologic variables
96 they considered were snowpack (maximum snow water equivalent and date of maximum SWE), annual stream-
97 flow volume, centroid timing (the date at which half the water year's flow has passed), and seasonal streamflow
98 volume; primary focus was on centroid timing, annual volume, and minimum 7-day flow. They did not examine
99 maximum daily flow. The purpose of this paper is to address this important gap in our understanding of the future
100 Northwest hydrology; to do so, we use the largest available ensemble of climate-hydrology scenarios. By using a
101 large ensemble, we ensure a reasonable breadth of climatic and hydrological futures in order to better describe the
102 range of possible future flooding and how it varies across the region with its diverse hydroclimates.

103 **2 Methods**

104 **2.1 Hydrologic modeling data set**

105 To assess changing flood magnitudes under climate change, we analyzed changes in water year maximum daily
106 flows in a large ensemble of streamflow simulations at 396 locations in the CRB (Figure MAP) and select water-
107 sheds in western Oregon and Washington (Chegwiddden et al., 2017). The simulations were constructed from

108 permutations of modeling decisions on forcing datasets and hydrologic modeling. Specifically, choices included
109 two RCPs (RCP4.5 and RCP8.5), ten GCMs, two methods of downscaling the climate model output to the reso-
110 lution of the hydrologic models, and four hydrologic model implementations, for a total of 160 permutations. For
111 our analysis, we extracted a more tractable dataset of 40 simulations per location, by only considering simulations
112 with RCP 8.5 and the Multivariate Adaptive Constructed Analogs (MACA) downscaling method (Abatzoglou
113 and Brown, 2012).

114

115 The rationale for using a subset of the available data is as follows. First, the time-dependent set of greenhouse gas
116 concentrations in RCP4.5 is fully included in RCP8.5, so any concentration of greenhouse gases on the RCP4.5
117 path can be converted to a point on RCP8.5 (at a different time). We analyzed results for both RCP8.5 and RCP4.5,
118 and found that to first order the changes in flood magnitude in RCP4.5 were approximately 2/3 those in RCP8.5,
119 which is also roughly the ratio of global temperature change over the period considered (IPCC Summary for
120 Policymakers, 2014). For clarity we show only the results for RCP8.5. Second, we considered only simulations
121 using the MACA downscaling method because of the method's ability to capture the daily GCM-simulated me-
122 teorology critical for assessing changes in extremes and its skill in topographically complex regions (Lute et al.,
123 2015). The other downscaling approach used by Chegwiddden et al. (2019), the Bias Correction and Statistical
124 Downscaling (BCSD) method (Wood et al. 2004), produces probability distributions of daily precipitation incon-
125 sistent with the GCM response to forcings because the method stochastically disaggregates monthly data to daily
126 data based on historical statistical properties of the daily data. This statistical property limits the ability of BCSD
127 to reproduce changes in storm frequency in the future, making it a less attractive choice for daily extreme flow
128 analysis (Hamlet et al. 2010; Guttman et al. 2014).

129

130 The GCMs used in this study are the CanESM2, CCSM4, CNRM-CM5, CSIRO-Mk3-6-0, GFDL-ESM2M,
131 HadGEM2-CC, HadGEM2-ES, Inmcm4, IPSL-CM5A-MR, and MIROC5. These ten GCMs were chosen primar-
132 ily for their ability to accurately reproduce observed climate metrics during the historical period mainly of the
133 Northwest US but also at sub-continental and larger scales as assessed in Rupp et al. (2013) and RMJOC (2018).
134 The four hydrologic model implementations originated from two distinct hydrologic models: the Variable Infil-
135 tration Capacity (VIC; Liang et al., 1994) model and the Precipitation Runoff Modeling System (PRMS; Leaves-
136 ley et al., 1983). VIC and PRMS are process-based, energy balance models and were both run on the same 1/16th
137 degree grid with output saved at a daily time step for the period 1950 to 2099. VIC is a macroscale semi-distributed
138 hydrologic model that solves full water and energy balances, and in these simulations it also included a glacier

139 model (Hamman & Nijssen, 2015). Three unique implementations of VIC were used with independently derived
140 parameter sets (P1, P2, P3) marked by differences in calibrated parameters, calibration methodology, and mete-
141 orological and streamflow reference sets. PRMS is a distributed, deterministic hydrologic model which, in con-
142 trast to VIC, does not allow for subgrid heterogeneity. See Chegwidden et al (2019) for details. It is important to
143 note that these hydrologic simulations and calibrations do not include reservoir models.

144 **2.2 Flood magnitude**

145 We assessed changes in flood magnitude in the Columbia River Basin by comparing maximum daily streamflows
146 over a 150-year period (1950-2100). We estimated the 10, 5, 2, and 1% probability of occurrence (commonly
147 referred to as the 10-, 20-, 50-, and 100-year flood, respectively) by fitting generalized extreme value (GEV)
148 probability distributions to simulated water year maximum daily flows for 50-year windows of the past (1950-
149 1999) and future (2050-2099) periods. (We also looked at 30- and 75-year windows, choosing 50 years as a
150 balance between sample size favoring longer periods, and nonstationarity considerations favoring shorter periods.)
151 We used Python’s `scipy.stats.genextreme` module (Jones et al., 2001) to fit a Gumbel distribution and estimate
152 flood magnitudes for each return period. We assessed change in flood magnitude as the “discharge ratio” of the
153 estimated future to past floods for a given return period; a ratio greater than 1 indicates an increase in flood
154 magnitudes while a ratio less than 1 indicates a decrease.

155
156 We describe how changes in flood magnitude vary by climatic zone across the PNW by using an efficient and
157 internally consistent proxy for climatic zone: the centroid of timing – the day in the water year that half the annual
158 volume of water has passed through the location. The centroid of timing is a metric of snow dominance (e.g.,
159 Stewart et al. 2005) which is related to the spatial distribution of temperature and tends to decrease downstream.
160 This temporal proxy of a hydrologic characteristic is effective in the Columbia Basin where most of the precipi-
161 tation occurs in winter and the relative magnitude and timing of the freshet from the spring thaw is a good indicator
162 of importance of snowmelt to streamflow. An early centroid indicates that rain, which falls predominantly during
163 the cooler, earlier part of the year, is the driver of the peak flows at the location, while a late centroid indicates
164 that snowmelt during later spring months is the prime hydrological driver. We computed the centroid using the
165 1950-79 simulated years. Note that Chegwidden et al. (2019) also used the *change* in centroid as a hydrologic
166 variable of interest; below, we discuss our results in the context of their findings.

167

168 **2.3 Verification**

169 Comparing directly between gauged flows and modeled flows is inadvisable since the flows are substantially
170 altered by regulation. However, a set of streamflows called No Reservoirs No Irrigation (NRNI; RMJOC 2017)
171 has been developed by federal agencies to support practical analysis. The NRNI dataset exists at ~190 sites across
172 the Columbia River Basin for the years 1950-2008, and are adjusted to correct for reservoir management and the
173 diversions and evaporation associated with both the reservoirs and with irrigated agriculture. This dataset is suit-
174 able for comparisons with our modeling setup, and we have computed return period curves at all the NRNI loca-
175 tions (not shown). On the lower mainstem Columbia, the return period curves are extremely close to those com-
176 puted from NRNI. Individual hydrologic model configurations are not consistently biased across the basin nor
177 across return periods; despite its different provenance, PRMS generally lies within the return period flows of the
178 three VIC configurations rather than being consistently different from all VIC configurations, except on the lower
179 Snake, where PRMS is consistently an outlier on the low end of the distribution. Only at Hills Creek in the
180 Willamette Basin do the modeled return period curves all lie outside NRNI, and only for the longest return periods
181 (>10 years).

182

183 We also examined the ensemble performance for 1950-2008 in the distribution of timing of peak daily flow for
184 28 locations along the Columbia, Snake, and Willamette. At all locations we examined, the median date (as well
185 as earliest and latest quartiles) of annual maximum flow in the ensemble is within 10 days of the observed, from
186 NRNI. The modeled distribution is a bit later than NRNI on the lower Columbia and a bit earlier than NRNI on
187 the Willamette. Note that the GCM simulations used to drive the hydrologic models during this verification period
188 are independent of the observed meteorology, so both the magnitude and the timing of annual maximum flows
189 are computed from first principles, and represent a remarkable agreement with observations. Although the mod-
190 eled flows are calibrated, the statistical approach to calibrations is not sensitive to the extreme maximum daily
191 flow studied here.

192

193 **3 Results**

194 **3.1 Regional changes in flood ratio**

195 Figure 3 shows the changes in maximum daily discharge for all of the 396 flow locations for different return
196 periods. The horizontal position of each circle represents the centroid of timing. The circles are semi-opaque so
197 overlapping circles lead to a deeper saturation. Points on the same river are ordered from more to less snow

198 dominant (i.e., right to left) traveling downstream; strings of circles in a smooth pattern usually indicate one of
199 the larger rivers, highlighted in Figure 4. Each circle in Figures 3 and 4 represents an average of 40 simulations:
200 10 GCMs and 4 hydrologic model configurations.

201
202 A striking result in Figure 3 is that, in contrast to the results of Tohver et al. (2014), the flood magnitude increases
203 (i.e., the discharge ratio exceeds one) at nearly every flow location and return period (though not for every indi-
204 vidual climate scenario, as shown in Figure 5). Broadly, the patterns are similar across all return periods though
205 with slightly higher ratios for longer return periods, and subsequent figures will show only the 10- and 100-year
206 floods. For the flow locations with centroid <125 or so (i.e. February 2), flood ratios are fairly concentrated about
207 1.25 for all return periods. For mixed rain-snow basins, roughly delineated by centroids between 125 and 160
208 (March 8 most years), flood ratios range widely from just below 1 to about 2.4 for the 10-year and 3.2 for 50- and
209 100-year floods. For the longer return intervals, there is a wide range of projected changes in daily flood at many
210 locations (indicated by the red coloring). This is undoubtedly partly due to the GEV fit extrapolating from 50 to
211 100 years. Finally, for the basins with flow centroid >160 , the ratios have a smaller range, from slightly greater
212 than 1 to a maximum that increases from about 2 for the 10-year, to about 2.75 for 100-year. Tohver et al. (2014)
213 distinguished basins by their DJF temperature, a rough proxy for our snow dominance metric, and found a sub-
214 stantial number of locations where the flood ratio for both 20-year and 100-year flood was as much as 20% lower
215 for the 2040s compared with a historical period. We return to this point in the conclusions.

216
217 To understand better how flood magnitude changes along the length of a river, we focus (Figure 4) on a handful
218 of significant rivers in the region: the mainstem Columbia, Willamette (along with major tributaries the McKenzie
219 and Middle Fork Willamette), and Snake, and also on the Chehalis in southwest Washington (see Introduction).
220 Flow locations are listed in Table 3 Rivers in the Appendix. Many of the larger tributaries also have flow points
221 in our dataset, so we can infer the role of tributaries in changing the flood magnitudes in the future, as discussed
222 below. The Columbia River includes the most snow-dominant basins, with a centroid of >190 days (early to mid
223 April) in the Canadian portion of the basin. The flood ratio decreases almost uniformly along the length of the
224 river, from 1.3 for the 10-year and >1.5 for the 100-year in the Canadian portion to just above 1 at the last few
225 points along the river (The Dalles, Bonneville, and Portland). Past flood events on the mainstem Columbia are
226 exclusively associated with large spring snowmelt, and the large tributaries (the Yakima, Snake, and Willamette)
227 contribute annual flow volume but rarely contribute peak flow at the same time; as shown below, the future flood
228 timing changes but flood magnitudes change little in the lower Columbia owing to the fact that the Columbia

229 integrates such diverse hydroclimates. Like the Columbia, the Willamette also has flood ratios that decrease along
230 the length of the river as it integrates more diverse hydroclimates, from 1.7 to 1.35 for both return periods. The
231 McKenzie River (points 15-17), one of the three tributaries that converge at Eugene to form the Willamette, is a
232 highly spring-fed river with higher baseflow than is represented in the hydrologic models, though it is unclear
233 how that difference would manifest in the flood statistics.

234

235 In contrast to the Columbia and the Willamette, the Snake behaves oppositely: flood ratio increases along the
236 length of the river, until the confluence with the Salmon River, which drains a large mountainous area of central
237 Idaho. On parts of the Snake the ratios are as high as 1.4 for 10-year and 1.6 for 100-year. Then after the confluence
238 with the Salmon River, which has much lower change in discharge ratio, the ratios on the Snake drop to about 1.2
239 for 10-year and about 1.3 for the 100-year. Our hypothesis is that in the Snake above the Salmon River, the
240 tributaries shift from snow-dominant to rain-dominant, so that a single storm can drive large rainfall-driven in-
241 creases (possibly with a snowmelt component) leading to larger synchronous discharges. The Salmon and Clear-
242 water rivers retain less exposure to such shifts, and dilute the effects of single large storms on flooding.

243

244 Each circle in Figures 3 and 4 represents an average of 40 simulations: 10 GCMs and 4 hydrologic model config-
245 urations. To better understand the range in results, Figure 5 shows the discharge ratio for all 40 simulations at
246 each point on the mainstem Columbia. Although the mean flood ratio at the lowest two points is only barely above
247 1, several ensemble members have ratios less than one, and a few have ratios >1.5. Moving upstream, the range
248 in results increases, as shown also by the color of the dots.

249 **3.2 Dependence of results on modeling choices**

250 As in Chegwiddden et al (2019), we separate the results - here for the three largest rivers - into variations across
251 GCM (Figure 6) and variations across hydrologic model configurations (Figure 7). The ranking of flood ratios by
252 GCM changes substantially between basins and even within a basin, and does not correspond to the changes in
253 seasonal precipitation. For the upper Columbia River, the models with the least warming - inmcm4 and GFDL-
254 ESM2M (Rupp et al 2017) - have almost no change in flood magnitude, but the HadGEM2-ES which warms
255 considerably in summer produces a large decrease in flood magnitude. In the Willamette and Snake Rivers, the
256 range of projected flood changes by different GCMs remains large from the headwaters to the mouth of the river,
257 whereas for the Columbia the range diminishes considerably as one moves downriver.

258

259 The variation of results depends less on hydrologic model than on GCM (Figure 7), though the differences across
260 hydrological models are still substantial. For the Willamette, lower Snake, and both upper and lower Columbia,
261 the PRMS model predicts substantially larger increases in flooding than the three calibrations of the VIC model.
262 For the upper Snake, it predicts substantially smaller change than any VIC calibration. While it is perhaps not
263 surprising that the three calibrations of VIC are close to each other, it is striking just how different are the projec-
264 tions from PRMS at most locations on these three rivers. Chegwidden et al. (2019) found that the main contrib-
265 utors to differences in hydrologic variables (except low flows) generally were the climate scenarios (GCM and
266 RCP), consistent with our findings here. (The order of models is similar in the equivalent figure for the 100-year
267 return period, but we elected to show the 10-year figure since the 100-year figure is more difficult to decipher
268 because the symbols overlap with those from other rivers.)

269
270 To parse the contributions of climate factors (represented by the GCMs) and hydrologic factors (represented by
271 the hydrologic models), we perform ANOVA on the 40 discharge ratios. The pie charts in Fig. 8 show the pro-
272 portion of the total variance explained by climate factors and hydrologic factors at different locations. For the
273 Willamette River, the portion of uncertainty connected to the climate grows more important and the portion of
274 uncertainty connected to the hydrologic variability less important going from the confluence of the three major
275 tributaries at Eugene to the mouth. For the Snake and Columbia rivers, climate is responsible for virtually all of
276 the variance in projections in the upper reaches, but only about half at the lowest point, similar to the Willamette.
277 The Willamette basin is much smaller, and a large storm can affect the entire basin on the same day, whereas
278 storms typically take a couple of days to move across the Snake and Columbia (and generally move up-
279 stream). With larger and more diverse contributing areas, differences in the rates with which the hydrological
280 models transfer precipitation to the point of interest become more important. Unlike Chegwidden et al. (2019),
281 we did not attempt to isolate the response to anthropogenic forcing from internal climate variability. Though
282 several techniques for separating these two factors have been used (e.g., Hawkins and Sutton, 2009; Rupp et al.,
283 2017; Chegwidden et al., 2019), these techniques are either infeasible with our dataset or we question their suita-
284 bility for the application to changes in extreme river flows.

285

286 **3.3 Change in timing**

287 Although in a broad hydrologic sense a flood is a flood regardless of what time of year it occurs, there are poten-
288 tially significant ecological differences depending on time of year; for example, scouring salmon redds (Goode et

289 al. 2013). Moreover, water management policies are strongly linked to the calendar year (see Discussion). We
290 computed the probability of flooding for (all 40) past and future simulations at all the points on the three rivers
291 (Figure 4) as a function of day of year (Figure 9). For the Willamette, no significant change in timing occurs;
292 however, for the upper Willamette, a single peak in likelihood in February becomes more diffuse. For the Snake,
293 all locations see a shift toward earlier floods, consistent with the transition to less snow-dominant and more rain-
294 dominant. Whereas floods were historically concentrated in the period of mid-May to mid-July, the projected
295 future flooding period spans December to June. For the Columbia, the mode in the flood timing shifts earlier by
296 half a month in the upper Columbia to about a month in the lower Columbia. The distribution also broadens with
297 an elongated tail towards winter such that there is low, but non-negligible, probability of floods occurring as early
298 as January. Although the magnitude of the 10- and 100-year flood events in the lower Columbia do not increase
299 much (Figures 4-7), the risk of major flood on any given day decreases, and the likelihood of major flooding in
300 May or April (or even February and March) increases.

301 **4 Discussion and conclusions**

302 Our study joins a small number of others in examining large hydroclimate ensembles. Gangrade et al. 2020 used
303 a similar ensemble approach analyzing hydrological projections for the Alabama-Coosa-Tallapoosa River Basin
304 with 11 dynamically downscaled and bias corrected GCMs (10 of which our studies share) and 3 hydrologic
305 models (including VIC and PRMS). While they did not examine extreme daily flows, they did calculate changes
306 in the 95% percentile of daily streamflow (Q95). Perhaps because of the hydroclimatic uniformity of that basin,
307 they found very small differences in Q95 across hydrologic models, which contrasts with our results showing
308 changes in flood magnitudes varying by watershed and distance downstream. Thober et al. (2018) conducted a
309 similar study in some European river basins, but rather than using a climate ensemble they simply imposed uni-
310 form warming scenarios on a hydrologic model (i.e. a more straightforward temperature sensitivity analysis rather
311 than an exploration of the range of future climate scenarios).

312
313 Returning to the Northwest, our findings contrast with earlier work. Salathe et al. (2014) found decreases in flood
314 magnitude at a substantial number of sites, but our results show increases in flood magnitude at nearly every
315 return period and location, which includes about 100 locations not included in their study. They also noted that
316 directly downscaling the GCM outputs leads to a smaller range of results than when running the regional model
317 as an intermediate step, so we infer that if we had had access to RCM simulations driven by all 40 of our GCMs,

318 our range of results might have been larger. Another important difference may be in the spatiotemporal coherence
319 of extreme precipitation, which in the RCM would be generated directly by the interaction of synoptic-scale
320 storms, topography, and to a small extent by surface water and energy balance; and in our study, by the interaction
321 of the GCM-scale synoptic storms and constructed analogs derived from observations. A large ensemble would
322 reduce the magnitude of that effect. In our study, the MACA statistical downscaling approach preserves much of
323 the daily variability from the GCM, so the primary reason for the difference between our results and theirs is
324 probably the fact that we analyzed 40 scenarios. Some locations, for example the points on the lower Columbia
325 river, had a handful of ensemble members with decreasing flood magnitude. But averaging the entire ensemble
326 nearly always resulted in an increase in flood magnitude. It is possible therefore that their study, repeated with a
327 larger ensemble of hydrologic-climate model combinations, might have found ubiquitous increases in flood mag-
328 nitude as ours did.

329
330 Prior results (Hamlet and Lettenmaier 2007, Tohver et al. 2014, Salathe et al. 2014) suggested a decrease in flood
331 magnitude in snowmelt-dominated basins like the Columbia, since reduced snowpack reduces the store of water
332 available to be released quickly in a spring flood (like the May-June 1948 Vanport flood). In a subbasin of the
333 Willamette, Surfleet and Tullos (2013) projected decreases in flood magnitude for return periods > 10 years in the
334 Santiam River basin under a high-emissions scenario (SRES A1B, 2070-2099 vs. 1960-2010; 8 GCMs), attrib-
335 uting the decreases to fewer large rain-on-snow events. Our results for the Santiam River show an *increase* of
336 40% for both 10- and 100-year floods; this result includes rain-on-snow events, since they are represented in VIC,
337 which computes the accumulation of water in the snowpack and determines whether sufficient energy has been
338 provided to create a melt event. Our results point to ubiquitous increases throughout the basin, even on the lower
339 mainstem Columbia. The coldest basins including the headwaters of the Columbia also had some large increases
340 in flood magnitude, suggesting that the former results were missing some key details. It seems likely that any
341 reduction in flood magnitude originating from the warming-induced reduction in spring snowpack is offset by the
342 increased pace of melt (including possibly rain-on-snow events). These results emphasize the necessity of revis-
343 iting reservoir rule curves, which are strongly tied to historical hydrographs, and also emphasize that changes in
344 the seasonality of flooding can be dramatically different from the changes in the mean hydrograph. In particular,
345 in the lower Snake and lower Columbia, changes in magnitude of flooding are modest but changes in timing of
346 the earliest quartile of flood events is much larger than the 0.5-1 month shift in the mean hydrograph.
347

348 A strength of our study compared with earlier studies is the use of a large ensemble, which samples a wide climate
349 space by using GCMs as opposed to RCMs. Conventional wisdom and evidence from the weather and seasonal
350 climate forecasting realms illustrate the utility of considering ensembles, and that generally the true outcome of a
351 prediction lies near the middle of the ensemble. Our ANOVA analysis (Figure 8) shows that climate scenarios
352 contribute a majority of the variation among results for most of the basin. Consequently, it is of great importance
353 to sample the climate scenarios broadly, which only GCMs can do. Large ensembles of RCMs are rare; the 12-
354 member NARCCAP ensemble (6 RCMs, 4 GCMs; Mearns et al. 2013), some of whose model runs were com-
355 pleted a decade ago, remains the largest, but has a spatial resolution of only 50km. CORDEX North America,
356 similarly now has a comparable-size ensemble, but mostly still at 50 km (some at 0.22°), and was not available in
357 such large numbers when we began our hydrologic simulations. At such spatial resolutions, RCMs would still
358 have to be further downscaled and bias corrected to use in our hydrologic models (~6km spatial resolution). In
359 the tradeoff between breadth of climate scenarios and spatial resolution, these ensembles offer insufficient im-
360 provement in spatial resolution relative to our GCM ensemble to justify sacrificing the breadth in climate scenarios
361 represented by choosing just 4 GCMs. While RCMs certainly have their place in such work and were used in
362 some previous studies, using GCMs in this study allowed for a larger climate space to be sampled, thus adding to
363 the robustness of our results.

364
365
366 The spread of results shown in Fig 5 suggests that although the likeliest outcome is little change in flood magnitude
367 in the lower Columbia, a prudent risk management strategy would consider the range of possibilities. However,
368 we view the highest outcomes (>50% increase in peak 100-yr flood) as less likely than other individual scenarios,
369 because they are the product of a hydrologic model that may be less suited to calculating the extreme changes in
370 a much warmer world.

371
372 Our findings provide an initial indication of how existing flood risk management could respond to a warming
373 climate. Reservoir management is guided by rule curves which are intended to reflect the changing priorities and
374 risks during the year. For example, reservoirs used for flood control have rule curves that require reservoir levels
375 to be lowered when approaching the time of year when flood likelihood increases, and reservoir levels may be
376 raised as the likelihood decreases. For the Willamette, we found little change in the distribution of timing of flood
377 events, which indicate that with the state of the science today, reservoir rule curves may need to be altered as to
378 magnitude of flooding (which our results indicate will increase by 30-40%) but not timing; a reservoir model

379 would be required for complete understanding of how flood risk (magnitude and timing) will actually change. For
380 the Snake, larger shifts in the timing imply a need to completely rethink the existing rule curves. For the Columbia,
381 the mode in flood timing shifts earlier by half a month in the upper Columbia to about a month in the low Colum-
382 bia. The distribution also broadens, with an elongated tail towards winter such that there is low, but non-negligible,
383 probability of floods occurring as early as January. These changes in timing imply a need for moderate alteration
384 of rule curves for reservoirs in the Canadian portion of the Columbia Basin.

385

386 Our results should not be taken as a precise prediction of flood magnitude change but rather as the best available
387 projections given the current state of the science. Two important factors need to be taken into account in inter-
388 preting our results: first, in using RCP8.5, we selected the most extreme emissions scenario. If efforts to stabilize
389 the climate before 2050 are successful, the flood magnitudes shown here will undoubtedly be smaller (our analysis
390 suggests most of the locations would see a change in flood magnitude about 1/3 smaller, for RCP4.5; e.g., a ratio
391 of 1.3 (30% increase) for RCP8.5 would correspond to a ratio of 1.2 for RCP4.5).

392

393 The second important factor in interpreting our results is that the actual river system in the Northwest includes
394 many dams, a majority of which have flood control as a primary (or one of a few top) objective. As a result, actual
395 flows (and the changes in flow) at a given point in the river would be altered by reservoir management. Translating
396 these changes in flood magnitude into actual changes would require a reservoir model for the basin or subbasin
397 of relevance. One could then compute optimal rule curves for the major flood control reservoirs (perhaps time-
398 evolving every couple of decades, to reflect the likely changes in scientific understanding and emissions trajec-
399 tory). Even without that additional analysis, however, our results stress that the magnitude and/or timing of flood
400 events will change throughout the basin. In other words, what worked for flood control in the past will not work
401 as well in the future.

402

403 This study may have some utility in framing and quantifying the possible changes in flood risk as the Columbia
404 River Treaty is in renegotiation, but further work would be needed to assign probabilities to future flood magni-
405 tude. Such work includes (a) understanding whether the PRMS projections of much larger change are reliable
406 (our analysis in section 2.3 shows that PRMS performs about as well as the three calibrations of VIC for simulating
407 past peak flows, but more work would be needed to understand the reasons for divergence in future projections),
408 (b) applying different statistical and/or dynamical downscaling methods, and (c) using a more sophisticated ap-

409 proach to evaluating extremes in a nonstationary climate (as advocated by Serinaldi and Kilsby, 2015). The mech-
410 anisms of flooding in the upper Columbia and elsewhere are also a key question arising from this work; this and
411 other work is needed to decipher the cause of the discharge ratio patterns we found along the major rivers. Fur-
412 thermore, a new generation of GCM outputs (CMIP6, Eyring et al. 2016) already has data available from over 25
413 GCMs; in the near future, it would be feasible to apply a newer multi-model hydrologic modeling approaches
414 (e.g., Clark et al., 2015) to the new generation of GCMs, though perhaps no significant changes would result.

415

416 Nonetheless, with current knowledge the fact that very few locations would see a decrease in flood risk under any
417 climate/hydrologic scenario is a strong statement of the need to update all aspects of flood preparation: the defi-
418 nition of N-year (especially 100-year) return period flows, flood plain mapping, and reservoir rule curves, to name
419 a few. Moreover, the challenges that the renegotiated Columbia River Treaty faces in accounting for climate
420 change now appear to include the necessity of incorporating the likely increase in flood risk throughout the region.

421

422 Generally, this study shows how complex the spatial and temporal patterns of change can be in a mixed rain-and-
423 snow basin. Basins of similar size and hydrological response to warming exist on most continents, so our results
424 provide a warning against using a small number of climate scenarios or a single hydrologic model to estimate
425 changes in flood risk in other basins.

426

427

428 **Code/data availability.** The data used here are available at <https://zenodo.org/record/854763>.

429

430 **Author contribution.** L. Queen performed all analyses, wrote portions of the text, and edited the document. P.
431 Mote guided the analysis and wrote much of the text. D. Rupp guided the analysis and edited the document. O.
432 Chegwiddden generated the underlying dataset, guided the analysis, provided assistance with programming, and
433 commented on the text. B. Nijssen generated the underlying dataset and commented on the text.

434

435 **Competing interests.** The authors declare no competing interests.

436

437 **Acknowledgments.** This project originated as a senior honors thesis by the first author, who thanks Hank Childs
438 of the University of Oregon for his mentorship. The research was supported by the NOAA Climate Impacts Re-
439 search Consortium, under award #NA15OAR4310145.

440

441
442
443
444
445
446
447
448
449
450
451
452
453
454
455
456
457
458
459
460
461
462
463
464
465
466
467
468
469
470

References

Berghuijs, W.R., R.A. Woods, C.J. Hutton, and M. Sivapalan, Dominant Flood Generating Mechanisms Across the United States. *Geophys. Res. Letts.*, 43, 4382-4390, doi: 10.1002/2016GL068070, 2016.

Byrd, J. G.: Calamity: The Heppner Flood of 1903. University of Washington Press, 2014.

Chegwidden, O. S., B. Nijssen, D.E. Rupp, and P.W. Mote, Hydrologic Response of the Columbia River System to Climate Change [Data set]. Zenodo. doi:10.5281/zenodo.854763, 2017.

Chegwidden, O. S., B. Nijssen, D.E. Rupp, J.R. Arnold, M.P. Clark, J.J. Hamman, S. Kao, et al: How Do Modeling Decisions Affect the Spread Among Hydrologic Climate Change Projections? Exploring a Large Ensemble of Simulations Across a Diversity of Hydroclimates. *Earth’s Future*, 7, 623–637, doi: 10.1029/2018EF001047, 2019.

Clark, M. P., Nijssen, B., Lundquist, J. D., Kavetski, D., Rupp, D. E., Woods, R. A., ... & Arnold, J. R. (2015). A unified approach for process-based hydrologic modeling: 1. Modeling concept. *Water Resources Research*, 51(4), 2498-2514.

Do, H. X., F. Zhao, S. Westra, M. Leonard, L. Gudmundsson, J. Chang, P. Ciais, D. Gerten, S.N. Gosling, H.M. Schmied, T. Stacke, B.J.E. Stanislas, and Y. Wada: Historical and Future Changes in Global Flood Magnitude – Evidence from a Model-Observation Investigation. *Hydrol. Earth Syst. Sci. Discuss*, doi: 10.5194/hess-2019-388, in review, 2019.

Douglas, E.M., R.M. Vogel, and C.N. Kroll: Trends in Floods and Low Flows in the United States: Impact of Spatial Correlation. *Journal of Hydrology*, doi: 10.1016/S0022-1694(00)00336-X, 2000.

471
472 Eyring, V., S. Bony, G.A. Meehl, C.A. Senior, B. Stevens, R.J. Stouffer, and K.E. Taylor: Overview of the Cou-
473 pled Model Intercomparison Project Phase 6 (CMIP6) Experimental Design and Organization. *Geosci. Model*
474 *Dev.*, 9, 1937-1958, doi: 10.5194/gmd-9-1937-2016, 2016.
475
476 Fritze, H., I.T. Stewart, and E. J. Pebesma: Shifts in Western North American Snowmelt Runoff Regimes for the
477 Recent Warm Decades. *Journal of Hydrometeorology*, doi: 10.1175/2011JHM1360.1, 2011.
478
479 Gangrade, Sudershan & Kao, Shih-Chieh & McManamay, Ryan. (2020). Multi-model Hydroclimate Projections
480 for the Alabama-Coosa-Tallapoosa River Basin in the Southeastern United States. *Scientific Reports*. 10.
481 10.1038/s41598-020-59806-6.
482
483 Goode, J.R., J.M. Buffington, D. Tonina, D.J. Isaak, R.F. Thurow, S. Wenger, D. Nagel, C. Luce, D. Tetzlaff, and
484 C. Soulsby: Potential effects of climate change on streambed scour and risks to salmonid survival in snow-domi-
485 nated mountain basins. *Hydrological Processes*, 27, 750-765, doi: 10.1002/hyp.9728.
486
487 Gutmann, E., T. Pruitt, M. P. Clark, L. Brekke, J.R. Arnold, D. A. Raff, and R.M. Rasmussen: An Intercomparison
488 of Statistical Downscaling Methods Used for Water Resource Assessments in the United States. *Water Resources*
489 *Research*, 50, 7167–7186, doi: 10.1002/2014WR015559, 2014.
490
491 Hamlet, A.F., and D.P. Lettenmaier: Effects of 20th Century Warming and Climate Variability on Flood Risk in
492 the Western U.S. *Water Resour. Res.*, 43, W06427, doi: 10.1029/2006WR005099, 2007.
493
494 Hamlet, A.F., P.W. Mote, M.P. Clark, and D.P. Lettenmaier, 2005: Effects of precipitation and temperature vari-
495 ability on snowpack trends in the western United States, *J. Climate*, 18, 4545–4561.
496
497 Hamlet, A.F., E.P. Salathé, and P. Carrasco: Statistical Downscaling Techniques for Global Climate Model Sim-
498 ulations of Temperature and Precipitation with Application to Water Resources Planning Studies. Chapter 4 in Fi-
499 nal Report for the Columbia Basin Climate Change Scenarios Project, Climate Impacts Group, Center for Science

500 in the Earth System, Joint Institute for the Study of the Atmosphere and Ocean, University of Washington, Seattle,
501 2010.

502

503 Hamman, J., and B. Nijssen: VIC 4.2.glaacier. Retrieved from <https://github.com/UW-Hydro/VIC/tree/sup->
504 [port/VIC.4.2.glaacier](https://github.com/UW-Hydro/VIC/tree/sup-port/VIC.4.2.glaacier), 2015.

505

506 Hawkins, E., and R. Sutton: The potential to narrow uncertainty in regional climate predictions. *Bulletin of the*
507 *American Meteorological Society*, 90, 1095–1108, doi: 10.1175/2009BAMS2607.1, 2009.

508

509 Kundzewicz, Z.W., S. Kanae, S.I. Seneviratne, J. Handmer, N. Nicholls, P. Peduzzi, R. Mechler, L.M. Bouwer,
510 N. Arnell, K. Mach, R. Muir-Wood, G.R. Brakenridge, W. Kron, G. Benito, Y. Honda, K. Takahashi, and B.
511 Sherstyukov: Flood Risk and Climate Change: Global and Regional Perspectives. *Hydrological Sciences Journal*,
512 59, 1-28, doi: 10.1080/02626667.2013.857411, 2014.

513

514 Lute, A. C., J.T. Abatzoglou, and K.C. Hegewisch: Projected Changes in Snowfall Extremes and Interannual Var-
515 iability of Snowfall in the Western United States. *Water Resources Research*, 51, 960–972, doi:
516 10.1002/2014WR016267, 2015.

517

518 Mearns, L.O., Sain, S., Leung, L.R. et al. Climate change projections of the North American Regional Climate
519 Change Assessment Program (NARCCAP). *Climatic Change* 120, 965–975 (2013).
520 <https://doi.org/10.1007/s10584-013-0831-3>.

521

522 Najafi, M.R., and H. Moradkhani: Multi-model Ensemble Analysis of Runoff Extremes for Climate Change Im-
523 pact Assessments. *Journal of Hydrology*, 525, 352-361, doi: 10.1016/j.jhydrol.2015.03.045, 2015.

524

525 River Management Joint Operating Committee: Climate and Hydrology Datasets for RMJOC Long-term Planning
526 Studies. Second edition: Part 1—Hydroclimate Projections and Analyses, retrieved from
527 <https://www.bpa.gov/p/Generation/Hydro/Pages/Climate-Change-FCRPS-Hydro.aspx>, 2018.

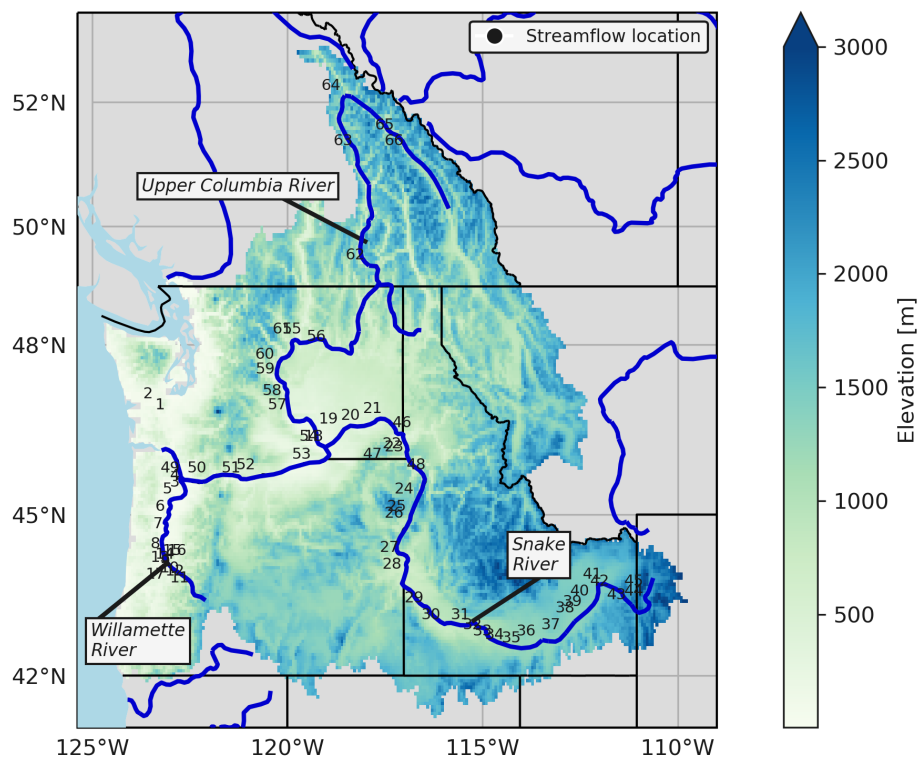
528

529 Rupp, D. E., J.T. Abatzoglou, K.C. Hegewisch, and P.W. Mote: Evaluation of CMIP5 20th Century Climate
530 Simulations for the Pacific Northwest USA. *Journal of Geophysical Research: Atmospheres*, 118, 10,884–10,906,
531 doi: 10.1002/jgrd.50843, 2013.
532
533 Rupp, D.E., J.T. Abatzoglou, and P.W Mote: Projections of 21st Century Climate of the Columbia River Basin.
534 *Clim. Dyn.*, doi: 10.1007/s00382-016-3418-7, 2016.
535
536 Salathé, E. P., et al: Estimates of Twenty-First-Century Flood Risk in the Pacific Northwest Based on Regional
537 Climate Model Simulations. *J. Hydrometeor*, 15, 1881–1899, 2014.
538
539 Serinaldi, F., and C.G. Kilsby: Stationarity is Undead: Uncertainty Dominates the Distribution of Extremes. *Ad-*
540 *vances in Water Resources*, doi: 10.1016/j.advwatres.2014.12.013, 2015.
541
542 Sharma, A., C. Wasko, and D.P. Lettenmaier: If Precipitation Extremes Are Increasing, Why Aren't Floods? *Wa-*
543 *ter Resources Research*, doi: 10.1029/2018WR023749, 2018.
544
545 Stewart, I. T., D.R. Cayan, and M.D. Dettinger: Changes Toward Earlier Streamflow Timing Across Western
546 North America. *J. Climate*, 18, 1136–1155, 2005.
547
548 Surfleet, C. G., and D. Tullos, D.: Variability in Effect of Climate Change on Rain-on-Snow Peak Flow Events
549 in a Temperate Climate. *Journal of Hydrology*, 479, 24-34, doi: 10.1016/j.jhydrol.2012.11.021, 2013.
550
551 Thober, S., Kumar, R., Wanders, N., Marx, A., Pan, M., Rakovec, O., Samaniego, L., Sheffield, J., Wood, E.F.
552 and Zink, M., 2018. Multi-model ensemble projections of European river floods and high flows at 1.5, 2, and 3
553 degrees global warming. *Environmental Research Letters*, 13(1), p.014003.
554
555 Tohver, I., A. F. Hamlet, and S.-Y. Lee: Impacts of 21st Century Climate Change on Hydrologic Extremes in the
556 Pacific Northwest Region of North America. *J. Amer. Water Resour. Assoc.*, doi: 10.1111/jawr.12199, 2014.
557
558 Vano, J. A., J. B. Kim, D. E. Rupp, and P. W. Mote: Selecting Climate Change Scenarios Using Impact-relevant
559 Sensitivities. *Geophys. Res. Lett.*, 42, 5516–5525, doi: 10.1002/2015GL063208, 2015.

560

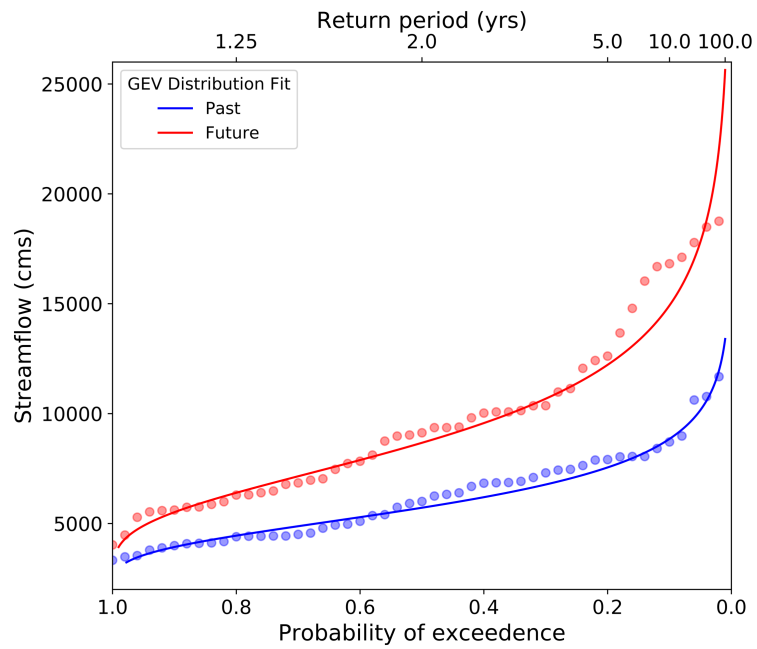
561 Wood, A., L. Leung, V. Sridhar, and D. Lettenmaier: Hydrologic Implications of Dynamical and Statistical Ap-
562 proaches to Downscaling Climate Model Outputs. *Clim. Change*, 62, 189–216, 2004.

563

565 **Figure captions**

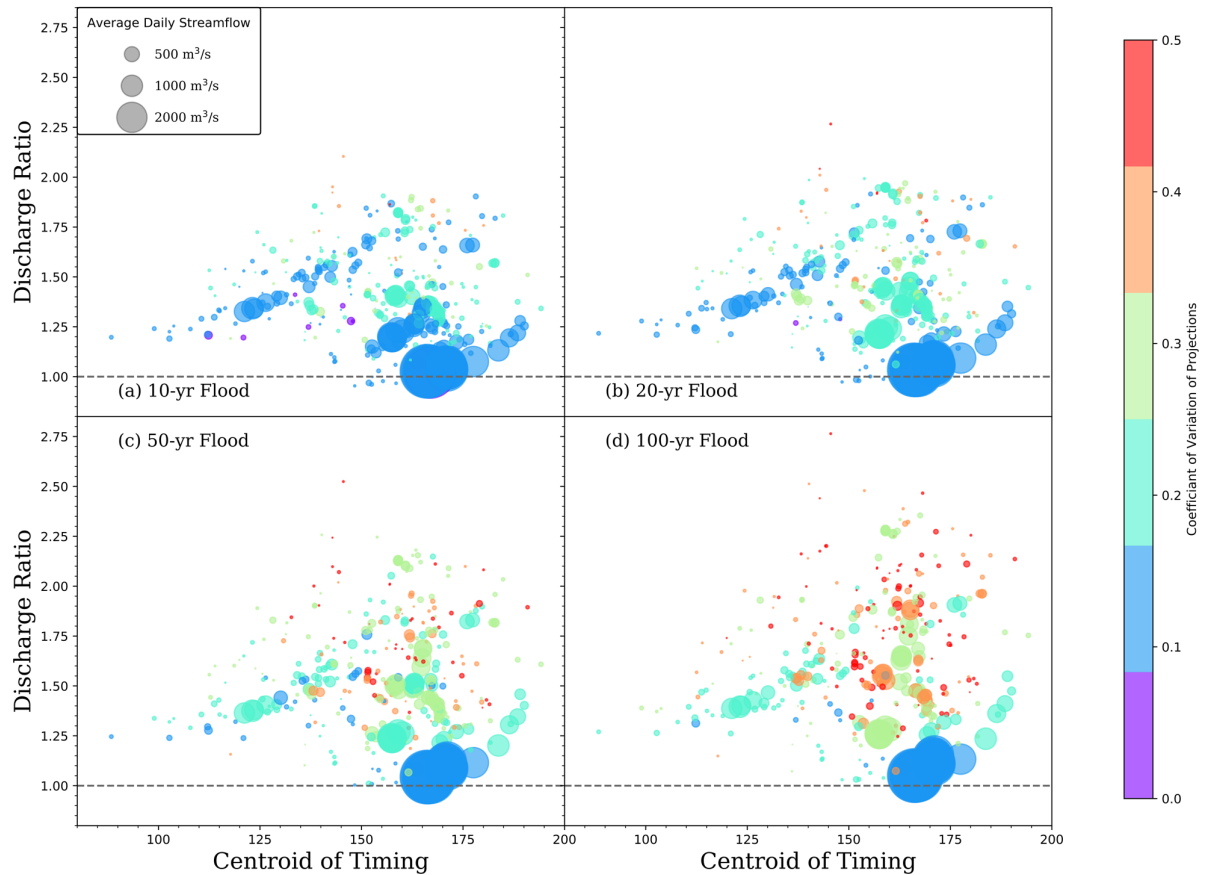
566

567 **Figure 1.** Domain of hydrologic simulations used in this paper, with colors indicating elevation of each grid cell,
 568 major rivers highlighted in blue, and numbers indicating locations of streamflow points highlighted in Figures 4-
 569 9, and Table 1. See Chegwiddden et al. (2017, 2019) for all streamflow locations plotted in Figure 3. Digital ele-
 570 vation data are in the public domain, obtained from <https://www2.usgs.gov/science/cite-view.php?cite=1530>



571

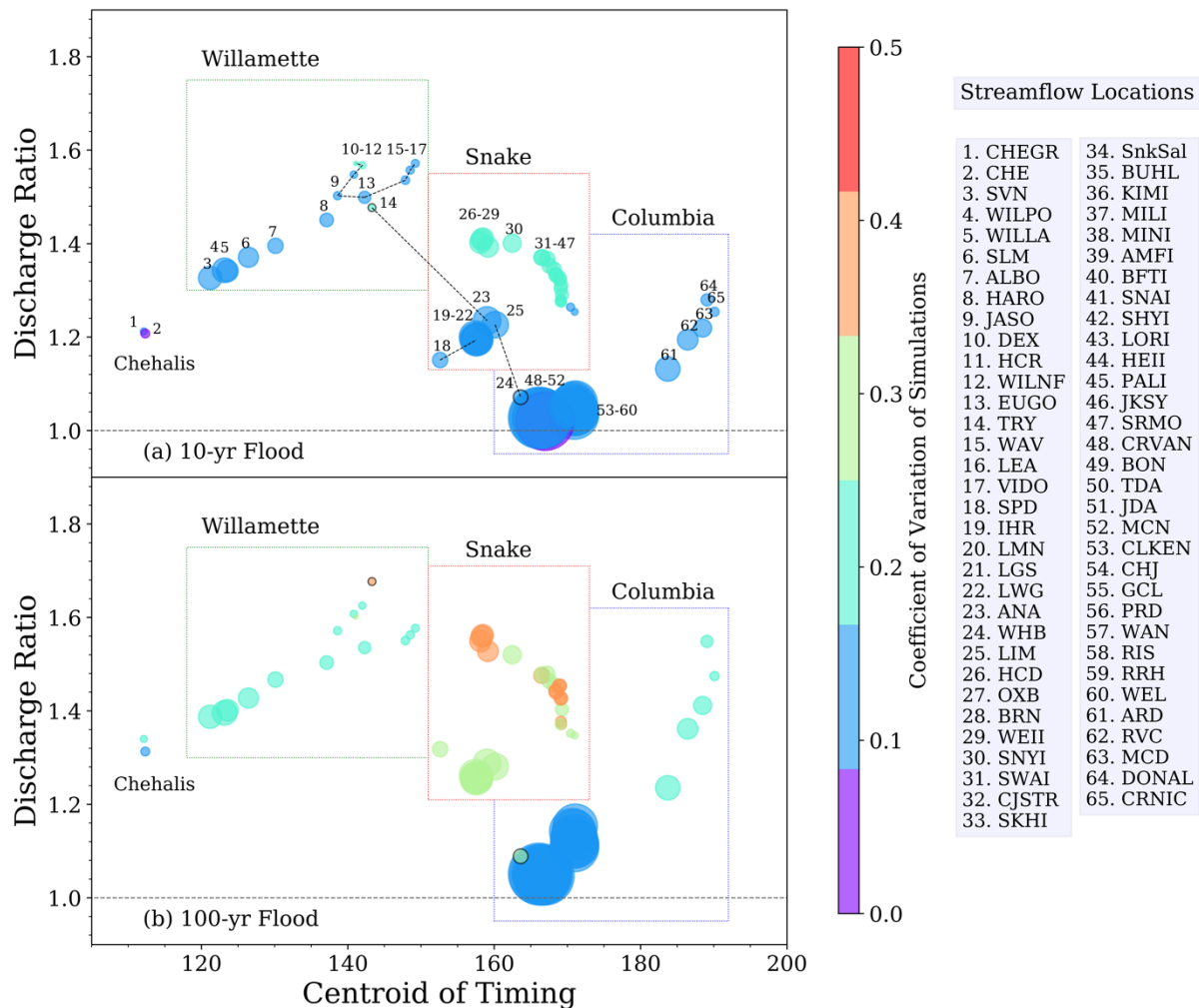
572 **Figure 2.** Generalized Extreme Value fit of annual maximum daily flow from 50 years of simulation using output
 573 from one GCM (HadGEM2-ES), one hydrologic model (PRMS), for the Willamette River at Portland. Red and
 574 blue dots/ lines indicate the annual values and GEV fit for the 1950-99 ‘past’ and 2050-99 ‘future’ periods.



575

576

577 **Figure 3.** Discharge ratios (future:past) versus centroid of timing (day on which 50% of water-year flow has
 578 passed, an indicator of snow dominance) for all 396 locations and four return periods. For each location, the
 579 average of 40 ensemble member ratios calculated from GEV distribution fitting from 50-year windows for the
 580 future (2050-2099) and past (1950-1999) time periods is shown. Points are sized by average daily streamflow and
 581 colored by the coefficient of variation of the 40 ratios.



583

584

585

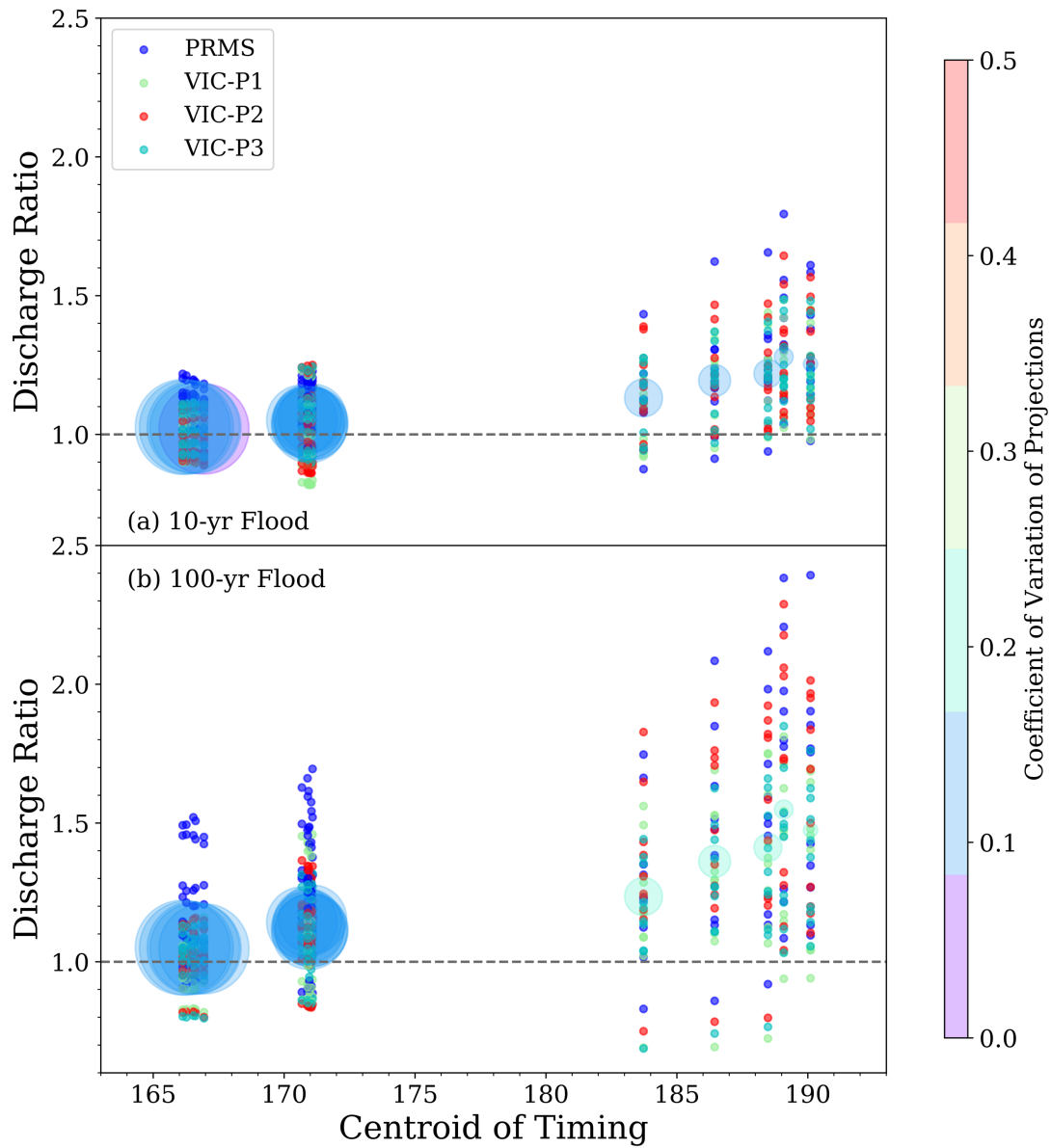
586

587

588

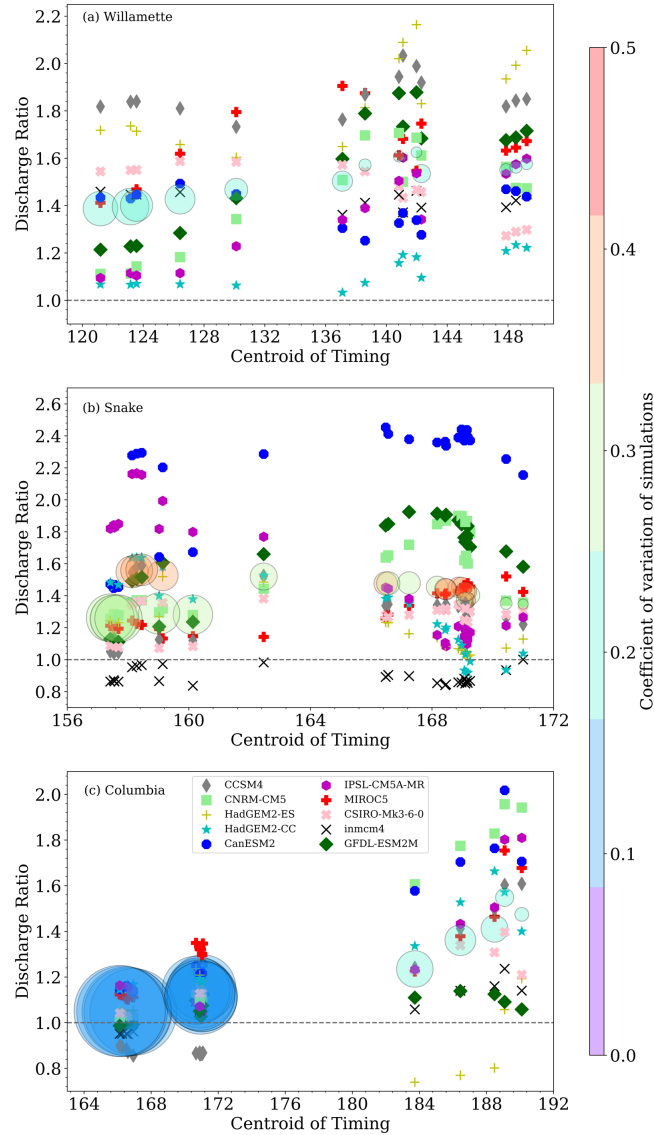
589

Figure 4. As in Figure 3 but only for points on the indicated rivers. Dashed lines indicate tributaries: 9-12 are on the Middle Fork Willamette, 15-17 on the McKenzie; tributaries of the Snake are the Grand Ronde (14), Clearwater (17) and Salmon (24). In the lower panel, the Grand Ronde and Salmon are clearly distinguished by a black circle around their perimeter. Table 1 translates the codes in the legend into named locations and shows the numerical values represented in the figure. As is evident from both snow-dominance and size, locations are ordered downstream to upstream from left to right for each river.

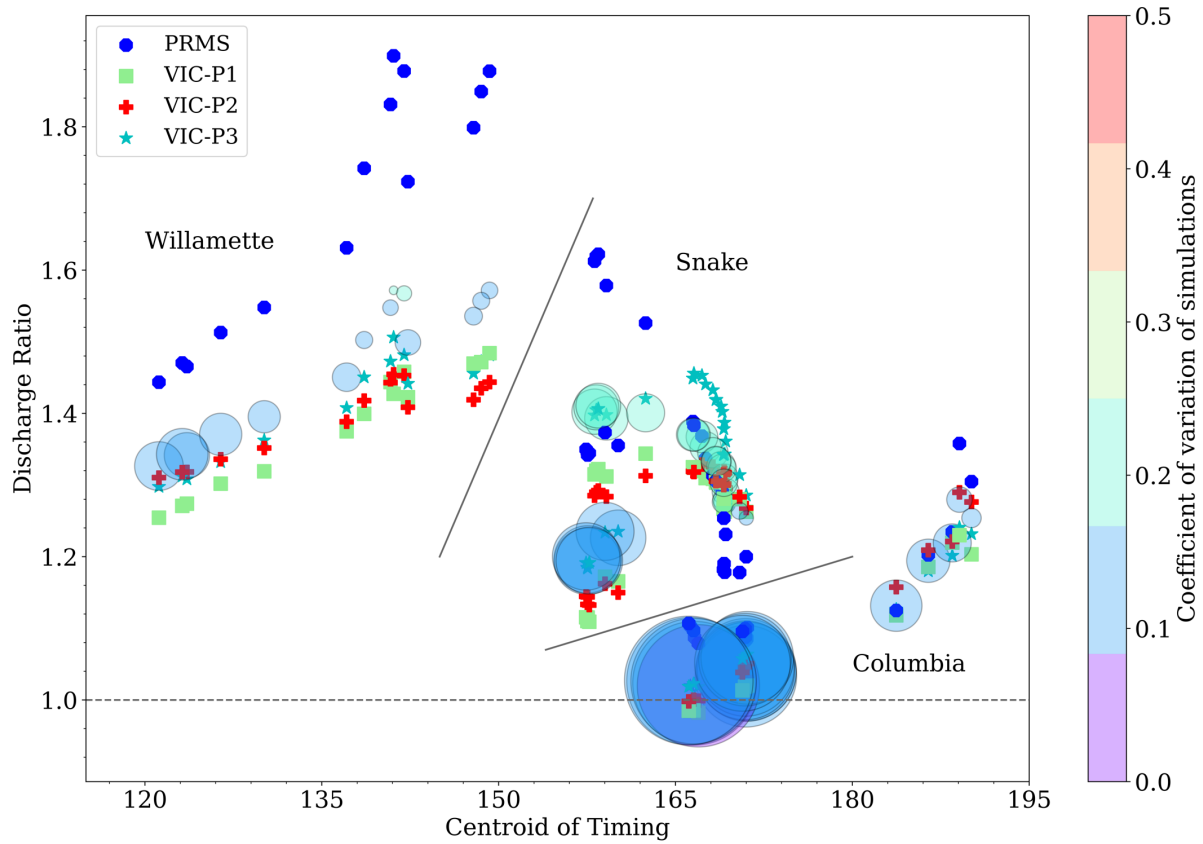


590

591 **Figure 5.** Averaged (large circles) and individual ensemble member (small colored circles) discharge ratios for
 592 simulated streamflow locations along the mainstem Columbia River for the 10-year (top) and 100-year (bottom)
 593 return periods. As shown in the legend, the color of the dots distinguishes results by hydrologic model setup.



594 **Figure 6.** Average ratios of all 40 ensemble members (large circles) and the average of 4 hydrologic model re-
 595 sults for each GCM (symbols), shown for simulated streamflow locations along the Willamette (top), Snake
 596 (middle), and the mainstem Columbia (bottom) for 100-year return periods. GCMs are ordered in the legend
 597 by their ranking in Rupp et al. (2017), representing their ability to simulate Northwest climate.



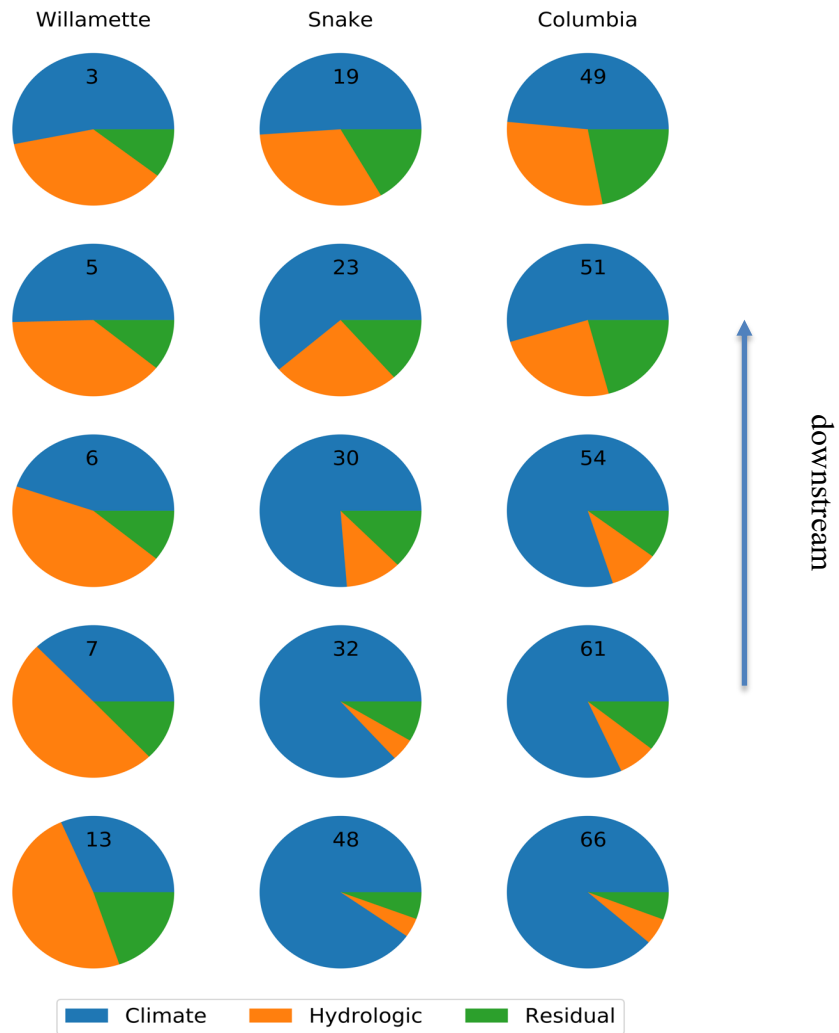
598

599

600

601 **Figure 7:** as in Figure 6 but averaged by hydrologic model, for 10-year return period, and combined into one

602 panel.



603 **Figure 8.** ANOVA results for select locations on the indicated rivers, for climate and hydrologic factors (and the
 604 residual). Charts are numbered to correspond with their location in Figure 4, with the most-downstream location
 605 at the top. The Snake enters the Columbia after location #54.

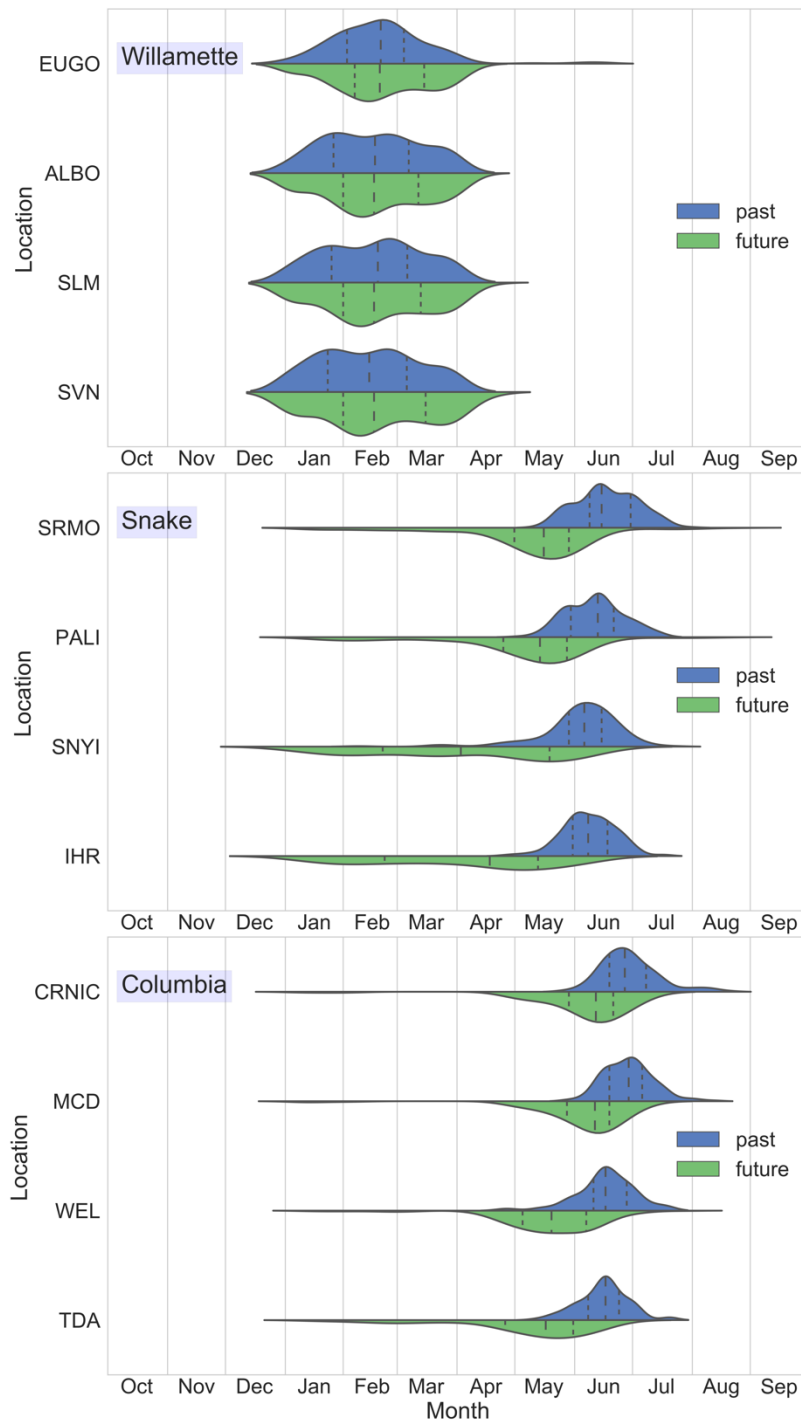


Figure 9. Statistical representations of the variation through the water year of the timing of flood events. For each of the 40 simulations, the dates of the 5 highest flows in the 50-year past (blue) and future (green) windows are tallied, and the resulting distributions smoothed. Long dashed lines indicate median date, short dashed lines the lowest and highest quartiles.

|607

608
609
610
611

Table 1 Information about locations featured in this paper - location, river, and discharge ratios

River	UW Key	Description	10-year flood discharge ratios				100-year flood discharge ratios			
			Avg.	Coeff. of Var.	Min	Max	Avg.	Coeff. of Var.	Min	Max
Chehalis	CHEGR	Chehalis R nr Grand Mount	1.21	0.09	1.03	1.42	1.34	0.18	0.87	2.07
Chehalis	CHE	Chehalis R at Porter	1.21	0.08	1.03	1.40	1.31	0.16	0.91	1.89
Willamette	SVN	T.W. Sullivan	1.33	0.09	1.07	1.64	1.39	0.22	0.87	2.39
Willamette	WILPO	Portland	1.34	0.09	1.08	1.69	1.40	0.23	0.86	2.47
Willamette	WILLA	Newberg	1.34	0.09	1.09	1.66	1.40	0.22	0.88	2.44
Willamette	SLM	Salem	1.37	0.09	1.10	1.70	1.43	0.22	0.84	2.52
Willamette	ALBO	Albany	1.40	0.09	1.11	1.73	1.47	0.20	0.89	2.40
Willamette	HARO	Harrisburg	1.45	0.10	1.18	1.86	1.50	0.22	0.88	2.37
Willamette	JASO	Middle fork @ Jasper	1.50	0.14	1.20	2.13	1.57	0.23	0.93	2.68
Willamette	DEX	Dexter	1.55	0.16	1.17	2.33	1.61	0.22	1.05	2.67
Willamette	HCR	Hills Creek	1.57	0.18	1.15	2.46	1.60	0.25	1.10	3.18

River	UW Key	Description	10-year flood discharge ratios				100-year flood discharge ratios			
			Avg.	Coeff. of Var.	Min	Max	Avg.	Coeff. of Var.	Min	Max
Willamette	WILNF	Oakridge	1.57	0.18	1.16	2.45	1.63	0.24	1.09	2.88
Willamette	EUGO	WR at Eugene (NWP)	1.50	0.12	1.26	2.04	1.54	0.22	0.88	2.57
Willamette	WAV	Walterville	1.54	0.13	1.29	2.13	1.55	0.18	1.04	2.23
Willamette	LEA	Leaburg	1.56	0.14	1.28	2.23	1.56	0.18	1.05	2.34
Willamette	VIDO	McKenzie nr Vida	1.57	0.15	1.28	2.32	1.58	0.19	1.02	2.41
Willamette	COT	Cottage Grove	1.25	0.11	0.97	1.69	1.39	0.29	0.78	2.38
Snake	IHR	Ice Harbor	1.20	0.13	0.92	1.75	1.26	0.28	0.79	2.84
Snake	LMN	Lower Monumental	1.20	0.13	0.92	1.76	1.26	0.28	0.78	2.77
Snake	LGS	Little Goose	1.19	0.13	0.92	1.77	1.26	0.28	0.78	2.83
Snake	LWG	Lower Granite	1.19	0.13	0.92	1.77	1.25	0.29	0.78	2.89
Snake	ANA	Anatone	1.24	0.14	0.95	1.74	1.29	0.29	0.78	2.84
Snake	LIM	Lime Point	1.23	0.14	0.94	1.73	1.28	0.30	0.76	2.81

River	UW Key	Description	10-year flood discharge ratios				100-year flood discharge ratios			
			Avg.	Coeff. of Var.	Min	Max	Avg.	Coeff. of Var.	Min	Max
Snake	HCD	Hells Canyon	1.40	0.18	1.01	2.11	1.55	0.38	0.87	3.62
Snake	OXB	Oxbow	1.41	0.18	1.01	2.11	1.56	0.38	0.86	3.65
Snake	BRN	Brownlee Dam	1.41	0.18	1.01	2.12	1.56	0.37	0.86	3.63
Snake	WEII	Weiser, ID	1.39	0.18	1.02	2.09	1.53	0.35	0.86	3.28
Snake	SNYI	Nyssa, OR	1.40	0.18	1.04	2.16	1.52	0.33	0.89	3.21
Snake	SWAI	Murphy, ID	1.37	0.19	0.98	2.09	1.48	0.33	0.84	3.24
Snake	CJSTR	CJ Strike Dam	1.37	0.19	0.97	2.08	1.48	0.32	0.86	3.08
Snake	SKHI	King Hill, ID	1.37	0.19	0.96	2.08	1.48	0.32	0.85	2.84
Snake	SNKBL WLSAL MON	Hagerman, ID	1.35	0.18	0.93	2.05	1.46	0.31	0.83	2.66
Snake	BUHL	Buhl, ID	1.35	0.19	0.91	2.05	1.46	0.32	0.73	2.54
Snake	KIMI	Kimberly, ID	1.33	0.19	0.89	2.03	1.44	0.33	0.74	2.47
Snake	MILI	Milner, ID	1.33	0.19	0.88	2.04	1.44	0.34	0.73	2.52

River	UW Key	Description	10-year flood discharge ratios				100-year flood discharge ratios			
			Avg.	Coeff. of Var.	Min	Max	Avg.	Coeff. of Var.	Min	Max
Snake	MINI	Minidoka, ID	1.33	0.19	0.86	2.02	1.45	0.33	0.70	2.53
Snake	AMFI	Neeley American Falls	1.32	0.19	0.85	1.99	1.45	0.34	0.67	2.69
Snake	BFTI	nr Blackfoot, ID	1.31	0.19	0.84	1.96	1.43	0.34	0.67	2.72
Snake	SNAI	nr Blackfoot, ID	1.30	0.19	0.84	1.95	1.43	0.34	0.67	2.69
Snake	SHYI	Shelley, ID	1.29	0.18	0.84	1.92	1.40	0.33	0.69	2.62
Snake	LORI	Lorenzo, ID	1.28	0.19	0.86	1.91	1.38	0.34	0.69	2.52
Snake	HEII	Heise, ID	1.28	0.18	0.86	1.91	1.37	0.33	0.70	2.53
Snake	PALI	Irwin Palisades	1.28	0.19	0.87	1.95	1.37	0.34	0.71	2.60
Snake	JKSY	Jackson, WY	1.26	0.15	0.89	1.73	1.35	0.30	0.80	2.46
Snake	SRMO	Moose, WY	1.25	0.13	0.91	1.59	1.35	0.25	0.83	2.34
Grand Ronde	TRY	Troy	1.48	0.19	1.09	2.55	1.68	0.34	1.01	4.38
Salmon	WHB	White Bird	1.07	0.13	0.83	1.57	1.09	0.33	0.72	2.81

River	UW Key	Description	10-year flood discharge ratios				100-year flood discharge ratios			
			Avg.	Coeff. of Var.	Min	Max	Avg.	Coeff. of Var.	Min	Max
Columbia	CRVAN	Vancouver	1.03	0.09	0.90	1.22	1.05	0.13	0.80	1.49
Columbia	BON	Bonneville	1.03	0.09	0.90	1.21	1.05	0.13	0.80	1.49
Columbia	TDA	The Dalles	1.03	0.08	0.90	1.20	1.05	0.13	0.81	1.52
Columbia	JDA	John Day	1.02	0.08	0.90	1.19	1.05	0.13	0.80	1.51
Columbia	MCN	McNary Dam	1.02	0.08	0.89	1.18	1.05	0.13	0.80	1.45
Columbia	CLKEN	Clover Island @ Kennewick	1.03	0.10	0.82	1.22	1.11	0.14	0.84	1.49
Columbia	CHJ	Chief Joseph	1.06	0.11	0.83	1.25	1.15	0.15	0.85	1.70
Columbia	GCL	Grand Coulee	1.06	0.11	0.83	1.25	1.14	0.14	0.84	1.66
Columbia	PRD	Priest Rapids	1.04	0.10	0.82	1.22	1.11	0.13	0.84	1.54
Columbia	WAN	Wanapum	1.04	0.10	0.82	1.22	1.11	0.14	0.84	1.58
Columbia	RIS	Rock Island	1.04	0.10	0.82	1.23	1.12	0.14	0.84	1.60
Columbia	RRH	Rocky Reach	1.05	0.10	0.83	1.23	1.13	0.14	0.84	1.61

River	UW Key	Description	10-year flood discharge ratios				100-year flood discharge ratios			
			Avg.	Coeff. of Var.	Min	Max	Avg.	Coeff. of Var.	Min	Max
Columbia	WEL	Wells Dam	1.05	0.10	0.83	1.24	1.14	0.14	0.85	1.63
Columbia	ARD	Hugh Keenleyside (Arrow)	1.13	0.12	0.87	1.43	1.24	0.21	0.69	1.83
Columbia	RVC	Revelstoke	1.19	0.12	0.91	1.62	1.36	0.23	0.69	2.08
Columbia	MCD	Mica Dam	1.22	0.12	0.94	1.66	1.41	0.24	0.72	2.12
Columbia	DONAL	Donald	1.28	0.14	1.02	1.79	1.55	0.25	0.94	2.38
Columbia	CRNIC	Nicholson	1.25	0.13	0.98	1.61	1.47	0.23	0.94	2.39
Clearwater	SPD	Spalding, ID	1.15	0.15	0.85	1.78	1.32	0.30	0.80	2.63
Clearwater	DWR	Dworshak Dam, ID	1.14	0.12	0.86	1.55	1.30	0.24	0.89	2.22
Santiam	JFFO	Santiam R nr Jefferson	1.40	0.10	1.14	1.81	1.41	0.25	0.81	2.27
Kootenay	COR	Corra Linn Dam, BC	1.08	0.12	0.85	1.31	1.15	0.16	0.79	1.67
Kootenai	LIB	Libby Dam, MT	1.17	0.14	0.92	1.52	1.32	0.22	0.85	2.01
Kootenay	BFE	Bonner's Ferry, ID	1.13	0.13	0.89	1.45	1.26	0.20	0.83	2.02

River	UW Key	Description	10-year flood discharge ratios				100-year flood discharge ratios			
			Avg.	Coeff. of Var.	Min	Max	Avg.	Coeff. of Var.	Min	Max
Pend Oreille	ALF	Albeni Falls, ID	1.26	0.14	0.96	1.68	1.65	0.30	1.02	2.97
Flathead	CFM	Columbia Falls, MT	1.24	0.13	0.94	1.63	1.65	0.26	1.01	3.19
Flathead	HGH	Hungry Horse Dam, MT	1.30	0.13	1.04	1.70	1.78	0.29	1.16	3.56
Yakima	KIOW	Yakima, WA	1.82	0.21	1.35	3.11	2.28	0.30	1.57	4.39

612